Available online at www.sciencedirect.com
ScienceDirect
Chinese Journal of Natural Medicines 2022, **20**(11): 873-880
doi: 10.1016/S1875-5364(22)60197-3
Chinese Journal of Natural Medicines

•Original article•

Construction and heterologous expression of the di-AFN A_1 biosynthetic gene cluster in *Streptomyces* model strains

WEI Weijia [1, 2Δ], WANG Wenzhao [1Δ], LI Chao [1, 2], TANG Yue [1], GUO Zhengyan [3], CHEN Yihua [1, 2*]

[1] *State Key Laboratory of Microbial Resources, Institute of Microbiology, Chinese Academy of Sciences, Beijing 100101, China;*
[2] *College of Life Sciences, University of Chinese Academy of Sciences, Beijing 100149, China;*
[3] *Institute of Medicinal Biotechnology, Chinese Academy of Medical Sciences, Beijing 100050, China*

Available online 20 Nov., 2022

[ABSTRACT] Natural cyclohexapeptide AFN A_1 from *Streptomyces alboflavus* 313 has moderate antibacterial and antitumor activities. An artificial designed AFN A_1 homodimer, di-AFN A_1, is an antibiotic exhibiting 10 to 150 fold higher biological activities, compared with the monomer. Unfortunately, the yield of di-AFN A_1 is very low (0.09 ± 0.03 mg·L^{-1}) in the engineered strain *Streptomyces alboflavus* 313_*hmtS* (*S. albo*/313_hmtS), which is not friendly to be genetically engineered for titer improvement of di-AFN A_1 production. In this study, we constructed a biosynthetic gene cluster for di-AFN A_1 and increased its production through heterologous expression. During the collection of di-AFN A_1 biosynthetic genes, the *afn* genes were located at three sites of *S. alboflavus* 313 genome. The di-AFN A_1 biosynthetic gene cluster (BGC) was first assembled on one plasmid and introduced into the model strain *Streptomyces lividans* TK24, which produced di-AFN A_1 at a titer of 0.43 ± 0.01 mg·L^{-1}. To further increase the yield of di-AFN A_1, the di-AFN A_1 BGC was multiplied and split to mimic the natural *afn* biosynthetic genes, and the production of di-AFN A_1 increased to 0.62 ± 0.11 mg·L^{-1} in *S. lividans* TK24 by the later strategy. Finally, different *Streptomyces* hosts were tested and the titer of di-AFN A_1 increased to 0.81 ± 0.17 mg·L^{-1}, about 8.0-fold higher than that in *S. albo*/313_hmtS. Successful heterologous expression of di-AFN A_1 with a remarkable increased titer will greatly facilitate the following synthetic biological study and drug development of this dimeric cyclohexapeptide.

[KEY WORDS] Cyclohexapeptide; di-AFN A_1; Titer improvement; Heterologous expression; *Streptomyces* host
[CLC Number] R284 **[Document code]** A **[Article ID]** 2095-6975(2022)11-0873-08

Introduction

Nonribosomal peptide (NRP) natural products display broad structural diversity and exhibit fascinating biological activities. Some of them have been applied as antibacterial, bioherbicidal, anticancer, and immunosuppressant agents [1-3]. Alboflavusins (AFNs) are a group of cyclohexapeptides from *Streptomyces alboflavus* 313 with moderate antibacterial and antitumor activity. The major component AFN A_1 is composed of an L-alanine, a D-valine, an unusual (2*S*,3a*R*,8a*S*)-3a-hydroxyhexahydropyrrolo-[2,3-*b*]indole-2-carboxylic acid (PIC), and three L- or D-piperazic acids (Piz) [4-6]. In a previous study, we proposed the biosynthetic pathway of AFNs, designed a 'better' antibiotic di-AFN A_1, the homodimer of AFN A_1 coupled by a biaryl linkage, and obtained di-AFN A_1 by expressing the cytochrome P450 enzyme HmtS, which catalyzes the C-C bond coupling of himastatin in *Steptomyces himastatinicus* ATCC 53653, into *S. alboflavus* 313 to construct *S. alboflavus* 313_*hmtS* (*S. albo*/313_hmtS) (Fig. 1) [7]. Specifically, di-AFN A_1 displays about 10 to 150 fold improvement in antibacterial and antitumor activity compared with AFN A_1, but the yield of di-AFN A_1 in *S. albo*/313_hmtS is fairly low. Moreover, chemical synthesis of such cyclopeptides and their homodimers [8, 9] are challengeable and not environmentally friendly [10], which precludes further investigation of di-AFN A_1 as a hit compound.

Metabolic engineering is frequently utilized for rapid and rational strain improvement, together with the traditional random mutagenesis [11] and medium optimization [12] methods. Unfortunately, *S. alboflavus* 313 is difficult to be genetically engineered, and we were never able to introduce more than one plasmid into it. With the advancement of synthetic biology toolboxes, heterologous reconstruction of the di-AFN A_1

[Received on] 24-Apr.-2022
[Research funding] This work was supported by the Ministry of Science and Technology of the People's Republic of China (No. 2020YFA0907703), the National Natural Science Foundation of China (Nos. 32070044, 32025002), and the Biological Resources Programme, Chinese Academy of Sciences (No. KFJ-BRP-009).
[*Corresponding author] E-mail: chenyihua@im.ac.cn
ΔThese authors contributed equally to this work.
These authors have no conflict of interest to declare.

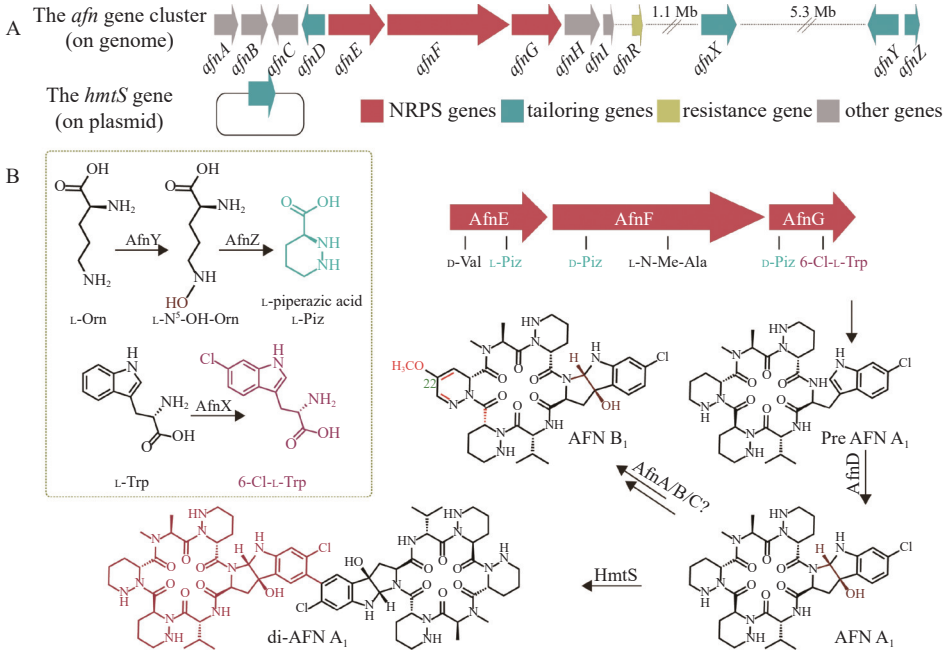

Fig. 1 Gene cluster and biosynthetic pathway of AFNs and di-AFN A_1. (A) The *afn* cluster on the genome of *S. alboflavus* 313. The *afnX* gene and the *afnY* and *afnZ* genes are about 1.1 Mb and 6.4 Mb away from the *afn* cluster, respectively. The *hmtS* gene is on the plasmid. (B) The proposed biosynthetic pathway of AFNs and di-AFN A_1

biosynthetic pathway in a model strain becomes a practical option, which can facilitate the following studies on titer improvement of di-AFN A_1 and prompt the generation of more di-AFN A_1 analogs by combinatorial biosynthesis or synthetic biology.

In this work, we first analyzed the genome of *S. alboflavus* 313 for the missing Piz synthesis genes. Then, we combined AFN A_1 biosynthetic genes and the coupling enzyme gene *hmtS* to construct a di-AFN A_1 biosynthetic gene cluster (BGC). Successful production of di-AFN A_1 was achieved by introducing a plasmid containing the BGC into *Streptomyces lividans* TK24, a model *Streptomyces* strain with plenty of genetic tools. Then, various strategies and host strains were tested to improve the titer of di-AFN A_1. The highest production was achieved in *Streptomyces coelicolor* M1154 (*S. coel*/pre_afn4), where the genes for non-proteinogenic amino acid supply were separated with the NRPS *afn* genes on an individual plasmid and the titer of di-AFN A_1 was about 8.0-fold higher than that in *S. albo*/313_hmtS.

Materials and Methods

Strains, media and reagents

Strains and plasmids used in this study are listed in Table S1. *Escherichia coli* DH10B was used for molecular cloning and plasmid propagation. *E. coli* S17-1 and *E. coli* ET12567/pUB307 were used for *E. coli-Streptomyces* conjugation. *E. coli* strains were cultured in Luria-Bertani (LB) broth (10 g·L^{-1} tryptone, 5 g·L^{-1} yeast extract, 10 g·L^{-1} NaCl, and 15 g·L^{-1} agar if needed) or grown on LB agar plates supplemented with appropriate antibiotics (50 mg·L^{-1} kanamycin, 25 mg·L^{-1} chloramphenicol, 50 mg·L^{-1} apramycin, and 50 mg·L^{-1} hygromycin). *S. alboflavus* 313 was cultured in Tryptic Soy Broth (TSB) medium (30 g·L^{-1} tryptic soy broth, BD) with 50 mg·L^{-1} apramycin for genomic DNA isolation. *Streptomyces* strains were grown on mannitol-soybean (MS) plates (20 g·L^{-1} soybean flour, 20 g·L^{-1} mannitol, and 20 g·L^{-1} agar) supplemented with appropriate antibiotics (50 mg·L^{-1} apramycin, 50 mg·L^{-1} hygromycin, and 50 mg·L^{-1} nalidixic acid) for spore preparation. To produce di-AFN A_1, *Streptomyces* strains were cultured and fermented in medium G (10 g·L^{-1} glucose, 3 g·L^{-1} peptone, 2.5 g·L^{-1} NaCl, 1 g·L^{-1} $CaCO_3$, pH 7.0).

General DNA manipulation

DNA synthesis and sequencing were performed in GenScript company (Nanjing, China). PCR was performed with PrimeSTAR Max DNA polymerase (Takara, Japan) or Taq DNA polymerase (Vanzyme, Nanjing, China). All primer oligos used in this study are listed in Table S2, while other DNA sequences, including promoter, insulator, RBS and gene expression cassette are listed in Table S3 (Supporting Information). Multisequence alignment was performed according to the ProbCons algorithm [13].

sgRNA template design and in vitro transcription

sgRNA were transcribed from dsDNA template with a size of 119 bp generated by overlap extension PCR with three primers [14]: one primer (X-sgRNA) containing the T7 promoter, 20-bp spacer sequence as well as 20-bp sequence complementary to the previous primer, and the other two (sgRNA-F and sgRNA-R) containing crRNA-tracrRNA chimera sequence of the sgRNA [15] as well as the complementary sequence to the previous primers. CHOPCHOP online server [16] was used to select the highest ranked spacer sequence in the

target BGC region. The PCR product was purified by HiPure PCR Pure Mini Kit (Magen, Guangzhou, China) according to the manufacturer instructions. *In vitro* transcription of each sgRNA was performed with HiScribe™ T7 Quick High Yield RNA Synthesis Kit (New England Biolabs (NEB), United States). Large quantities of sgRNAs were purified using the RNApure Rapid RNA Kit (BioMed, Beijing, China). The sgRNAs were diluted with RNase-free water and stored at −20 °C until use.

Cloning of the afn gene cluster

Part of the *afn* gene cluster (accession No. MH497044) from *S. alboflavus* 313 was directly cloned for AFN A_1 biosynthesis according to the previously described CATCH method [17]. The sgRNAs were obtained by *in vitro* transcription. For isolation of *S. alboflavus* 313 genomic DNA (gDNA), the mycelia were collected after two-day cultivation in TSB media at 28 °C, 220 r·min^{-1} and the gDNA was extracted using the salting-out method as described [18]. Cas9 digestion of *S. alboflavus* 313 gDNA using sg-DG-F and sg-DG-R (generated through overlap extension of sgRNA-DG-F/sgRNA-DG-R, guide RNA-F plus guide RNA-R) was conducted in a 200 μL reaction mixture containing 10 μg gDNA, 20 μL 10 × NEBuffer 3.1, 5 μL Cas9 (GeneCopoeia, Germany), and 5 μg of each sgRNA. The reaction mixture was incubated at 37 °C for 2 h. The digested DNA was precipitated with ethanol and resuspended in 20 μL DNase-free water. The linearized capture vector pPAB was amplified using the primers Fw-PV/Rv-PV, which contained a 30 bp overlap sequence to the target sequence. Around 50 ng of the pPAB backbone and 1 μg of digested genome fragments were assembled using the Gibson assembly method. The correct clones were verified by PCR using the VF-B1/VR-B1 and VF-B2/VR-B2 primers and named as pPAB_afn1.

Insertion of constitutive promoters between afnD and afnE

The pPAB_afn1 plasmid was digested with Cas9 guided by sg-ep-F and sg-ep-R (generated through overlap extension of sgRNA-ep-F/sgRNA-ep-R, guide RNA-F plus guide RNA-R). The exchanged promoter-insulator [19] sequence plus homologous arms were synthesized (RiboJ10-*ermE*p-P21-LtsvJ) and ligated with the recovered pPAB_afn1 fragment by Gibson assembly to generate pPAB_afn1.1.

Re-cluster the precursor and tailoring genes to construct the di-AFN A_1 biosynthetic gene cluster

We constructed *hmtS/afnR* and *afnX/Y/Z* expression cassettes and then put them together with the *afn* cluster to afford the di-AFN A_1 biosynthetic gene cluster. Briefly, the *kasO*p* promoter and a synthetic RBS (RBSH) generated by RBS Calculator [20] were synthesized, while the 1.2-kb *afnR* gene and the 1.2-kb *hmtS* gene were amplified by PCR with primers Fw-R/Rv-R from *S. alboflavus* 313 and primers Fw-h/Rv-h from *S. himastatinicus* ATCC 53653, respectively. The *kasO*p*-RiboJ-RBSH-*hmtS-afnR* expression cassette was obtained through overlap PCR using primer pair Fw-H/Rv-H and then inserted to pPAB_afn1.1 plasmid that was digested with Cas9 guided by sg-H-F/sg-H-R (generated through overlap extension of sgRNA-H-F/sgRNA-H-R, guide RNA-F plus guide RNA-R) by Gibson assembly to generate the pPAB_afn1.2.

The 1.6-kb *afnX* (accession No. MH497045), 0.6-kb *afnY*, and 1.3-kb *afnZ* (Table S3) containing fragments were amplified with primer pairs Fw-X/Rv-X, Fw-Y/Rv-Y, and Fw-Z/Rv-Z, respectively, from *S. alboflavus* 313. The SPL44 promoter and a synthetic RBS (RBSX) for the expression of *afnX/Y/Z* cassette was synthesized (SPL44-RBSX). The linearized vector was amplified from plasmid pRG with primers Fw-RV/Rv-RV. These DNA segments were assembled through the Gibson assembly method to generate plasmid pRGP_pre. The pPAB_afn1.2 plasmid was digested with Cas9 guided by sg-pre-F/sg-pre-R (generated through overlap extension of sgRNA-pre-F/sgRNA-pre-R, guide RNA-F plus guide RNA-R). The *afnX/Y/Z* expression cassette was amplified using primer pair Fw-Pre/Rv-Pre and ligated with the recovered pPAB_afn1.2 fragment by Gibson assembly to generate plasmid pPAB_afn2 that harboring all genes for di-AFN A_1 biosynthesis.

Construction of the multiple site-specific integrase expression cassettes

Given that the pPAB backbone already has a φC31-*attP*^{φC31} system, another two *Att/Int* systems, TG1/VWB1 and corresponding *attP* sites were chosen to multiply the copy number of the di-AFN A_1 BGC in *Streptomyces*. The TG1/VWB1 expression cassette including TG1-*attP*^{TG1} and VWB1-*attP*^{VWB1} was synthesized and ligated with the recycled pPAB_afn2 fragment, which was digested with Cas9 by the guidance of sg-int (generated through overlap extension of sgRNA-int, guide RNA-F plus guide RNA-R), to generate the plasmid pPVTAB_afn3.

Splitting of the di-AFN A_1 BGC into two plasmids

The complete di-AFN A_1 BGC was divided into two plasmids, pPAB_afn4 and pTHS_pre. To construct plasmid pPAB_afn4, the *afnX/Y/Z* genes were excised from plasmid pPAB_afn2 with Cas9 guided by sg-De-F and sg-De-R (generated through overlap extension of sgRNA-De-F and sgRNA-De-R, guide RNA-F plus guide RNA-R). The remaining backbone of pPAB_afn2 was reassembled with a synthesized homologous sequence (JS) to generate pPAB_afn4. To construct plasmid pTHS_pre, the *afnX/Y/Z* cassette was amplified from plasmid pPAB_afn2 with primer pair Fw-pre/Rv-pre and the linearized pTHS vector was obtained by PCR with primer pair Fw-TV/Rv-TV. The two DNA fragments were assembled through the Gibson assembly method to yield the pTHS_pre plasmid.

Construction of the di-AFN A_1 BGC expressing strains

E. coli S17-1 containing the plasmids containing the di-AFN A_1 BGC was used as the donor strain for conjugation to *S. lividans* TK24 and *Streptomyces albus* J1074. Using plasmid pPAB_afn2 as an example, plasmid pPAB_afn2 was transferred into *E. coli* S17-1 and then conjugated into *S. lividans* TK24 to generate *S. livi*/afn2. Similarly, *E. coli-Streptomyces* conjugation was carried out to obtain *S. livi*/afn3, *S.*

livi/pre_afn4, and *S. albu*/pre_afn4. As *S. coelicolor* M1154 possess a potent methyl-specific restriction system, the methylation deficient strain *E. coli* ET12567/pUB307 containing the plasmid with the di-AFN A_1 BGC was adopted as the donor strain and conjugated to *S. coelicolor* M1154 to generate *S. coel*/pre_afn4. To confirm the full integration of the di-AFN A_1 BGC on the genomes of these model *Streptomyces* strains, primer pairs VF-N1/VR-N1, VF-N2/VR-N2, VF-N3/VR-N3, VF-D/VR-D, VF-H/VR-H, VF-X/VR-X, and VF-YZ/VR-YZ were used to verify the presence of *afnE*, *afnF*, *afnG*, *afnD*, *hmtS*, *afnX*, and *afnY/Z*, respectively. Primer pairs VF-Phi/VR-Phi, VF-VWB/VR-VWB, and VF-TG1/VR-TG1 designed adjacent to the corresponding *attB* and *attP* sites of integrase φC31, VWB, and TG1, respectively, were used to confirm the copy number of *afn* gene cluster on the genome of the corresponding *Streptomyces* strains.

Production and detection of Di-AFN A_1

For the production of di-AFN A_1, a loop of *Streptomyces* spores was inoculated into a 250 mL flask with 50 mL medium G and the corresponding antibiotics, and cultured at 28 °C, 220 r·min^{-1} for 36 h for seed culture preparation. The seed culture was inoculated (10% *V/V*) into 250 mL flasks containing 50 mL medium G and the corresponding antibiotics and then cultured under the same conditions for five days. Then, the culture broth was extracted with a two-fold volume of ethyl acetate and concentrated at 28 °C in *vacuum*. The resultant sample was re-dissolved in 1 mL methanol and subjected to HPLC analysis, which was carried out on a Shimadzu HPLC system (Shimadzu, Japan) using an Apollo C_{18} column (5 μm, 4.6 mm × 250 mm, Alltech, United States) with acetonitrile and water containing 0.1% trifluoroacetic acid as the mobile phase. The concentration of acetonitrile was changed from 15% to 50% over 5 min, increased to 87% over 20 min, then maintained at 87% for 5 min, and increased to 100% over 5 min. The flow rate was 1 mL·min^{-1}, and the detection wavelength was 220 nm.

Statistical analysis

A calibration curve was plotted using AFN A_1 and di-AFN A_1 standards [7] isolated in our lab. The concentrations were calculated based on their corresponding peak area under HPLC trace.

Data were analyzed by GraphPad Prism 9 and presented as mean ± standard deviation. Statistical significance was analyzed by Student's *t*-test, with **** $P < 0.0001$.

Results and Discussion

Genes for di-AFN A_1 biosynthesis

S. alboflavus 313 produces not only the A series AFNs represented by AFN A_1, but also the B series AFNs with a C_{22}-methoxyl group (Fig. 1). It was proposed that the three genes encoding NRPSs *afnE*, *afnF*, and *afnG* and the *afnD* gene encoding a P450 enzyme are essential for AFN A_1 biosynthesis; the other three structural genes *afnA* (encoding a P450 oxidase), *afnB* (encoding a methyltransferase), and *afnC* (encoding a methyltransferase) are possibly involved in the following tailoring steps, affording the B series AFNs.

In addition to the four structural genes (*afnD/E/F/G*), genes for non-proteinogenic amino acid (PIC and Piz) synthesis are also needed for AFN A_1 construction. The tricyclic PIC moiety was proposed to be derived from 6-Cl-L-Trp, which is converted from L-Trp by AfnX, an FAD-dependent halogenase encoded by a gene about 1.1 Mb away from the *afn* gene cluster. The biosynthesis of the unusual Piz moiety was well elucidated in kutznerides. An *N*-hydroxylase, KtzI, converted L-Ornithine (L-Orn) to L-N^5-OH-Orn [21], which was further modified by a hemoenzyme, KtzT, to form L-Piz [22]. Genes converting L-Orn to L-Piz usually clusters with the structural genes of Piz-containing natural products on microbial genomes. However, no such genes have been found within or flanking the *afn* gene cluster. Careful *in silico* analysis of the genome of *S. alboflavus* 313 revealed two adjacent genes, *afnY* and *afnZ*, for Piz synthesis. AfnY displayed high similarities with the characterized L-Orn *N*-hydroxylases KtzI (59.40% identity, GenBank: ABV56589.1) and HmtM (61.67% identity, GenBank: CBZ42147.1). Meanwhile, AfnZ exhibited 56.07% identity with KtzT (GenBank: ABV56600.1) and 70.09% identity with HmtC (GenBank: CBZ42137.1), the two identified oxidases converting L-N^5-OH-Orn to L-Piz. It should be noted that *afnY* and *afnZ* are located about 6.4 Mb away from the *afn* gene cluster. Thus, the genes for AFN A_1 biosynthesis are separated to three sites on *S. alboflavus* 313 genome (Fig. 1A).

As aforementioned, the P450 oxidase gene, *hmtS*, from *S. himastatinicus* ATCC 53653 is needed for coupling AFN A_1 to di-AFN A_1 by a C-C bond forming biaryl linkage between the PIC moieties. To protect the hosts from the toxicity of AFN_1 and di-AFN_1, we analyzed the *afn* gene cluster with antiSMASH [23] and found a candidate resistance gene *afnR* (encoding a major facilitator transporter) downstream of the *afnG* gene. Introduction of cellular resistance genes to a heterologous host has been frequently used in the heterologous expression of natural products [24, 25].

Expression of the di-AFN A_1 BGC in S. lividans TK24

To construct the gene cluster for di-AFN A_1 heterologous production, we cloned a 26-kb DNA fragment containing the *afnD/E/F/G* genes from *S. alboflavus* 313 genome to the pPAB vector to generate pPAB_afn1 using the CATCH method (Fig. 2A). Then, the regulatory network of the *afn* gene cluster was refactored by inserting a constitutive P21 promoter plus a RiboJ insulator in front of *afnD* and a constitutive *ermE*p promoter plus an LtsvJ insulator to control the *afnE/F/G* operon. The non-proteinogenic amino acid *afnX/Y/Z* operon for PIC and Piz supply was placed at the downstream of the *afnE-G* operon and controlled by a constitutive SPL44 promoter. Meanwhile, the *hmtS* gene and *afnR* gene were driven by a strong *kasO*p* promoter and placed at the downstream of the *afnD* operon. The resultant plasmid pPAB_afn2 (Fig. 2B) was introduced into a model *Streptomyces* strain *S. lividans* TK24 to generate S. *livi*/afn2

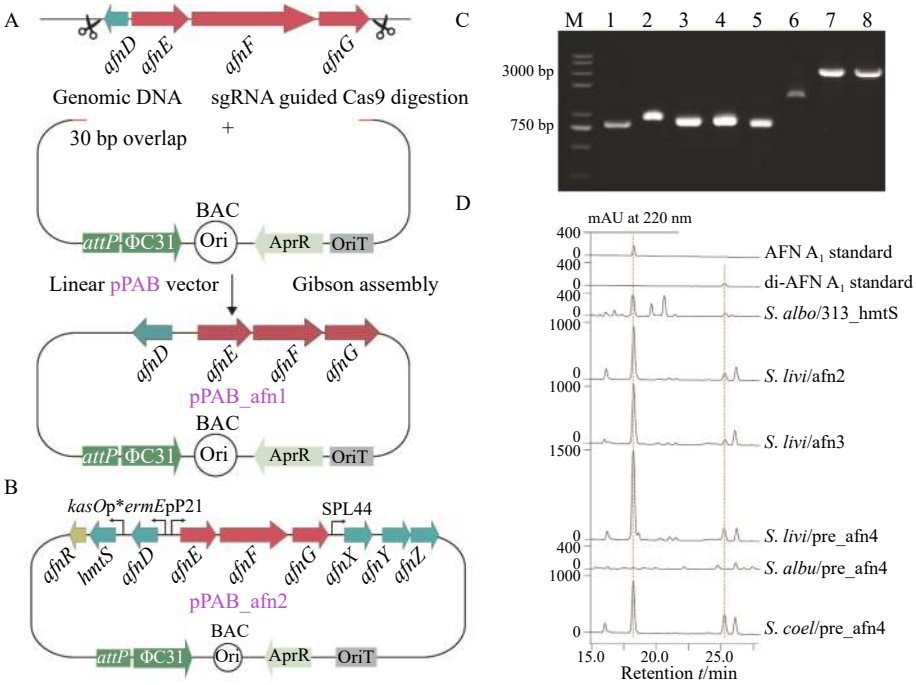

Fig. 2 Construction of the di-AFN A_1 BGC and its heterologous expression in *S. lividans* TK24. (A) A sketch map of cloning the *afn* gene cluster using the CATCH method. (B) Construction of the di-AFN A_1 BGC. *hmtS*, *afnD*, *afnE/F/G*, and *afnX/Y/Z* are under the control of functionally defined transcriptional activation elements. (C) PCR verification of the integration of the di-AFN A_1 BGC on the genome of *S. lividans* TK24. M, marker; Lane 1, verification of the integration of the di-AFN A_1 BGC to the *attB*$^{\varphi C31}$ landing site; Lanes 2 to 8, verification of the existence of *afnE, afnF, afnG, afnD, hmtS, afnX*, and *afnY/Z*. (D) HPLC detection of AFN A_1 and di-AFN A_1 in the heterologous expression strains

through *E. coli-Streptomyces* conjugation, and the correct ex-conjugate was verified by PCR (Fig. 2C). Using the *S. albo*/313_hmtS as a positive control, we fermented these two strains in medium G for five days. To our delight, both AFN A_1 and di-AFN A_1 were synthesized in *S. livi*/afn2 as well as in *S. albo*/313_hmtS. The AFN A_1 yield in *S. livi*/afn2 was 2.54 ± 0.15 mg·L^{-1}, about 1.4-fold higher than that in *S. albo*/313_hmtS (1.08 ± 0.33 mg·L^{-1}), while the yield of di-AFN A_1 in *S. livi*/afn2 was 0.43 ± 0.10 mg·L^{-1}, about 3.8-fold higher than that in *S. albo*/313_hmtS (0.09 ± 0.03 mg·L^{-1}) (Fig. 2D). These findings demonstrate the excellent performance of heterologous production of valuable compounds by synthetic biological means.

Multiplying the copy number of BGC to improve di-AFN A_1 titer

Previous researches indicated that increasing the copy number of BGC significantly can improve compound titers [26]. Tandem amplification of the copy number of actinorhodin BGC to 4−12 resulted in about 20-fold improvement in the yield of actinorhodin, compared with the original host [27]. By increasing the spinosad BGC to five copies in the heterogolous host *S. coelicolor* M1146, the yield of spinosad increased about 224-fold compared with the parent strain [28]. Guided by the concept of "multiple integrases and multiple *attB* sites", LI *et al*. [29] developed the advanced multiplex site-specific genome engineering (aMSGE) method. As a proof of concept, they magnified the 5-oxomilbemycin BGC up to four copies in *S. hygroscopicus* and the yield was about 1.8-fold higher than that in the wild-type strain. The aMSGE method does not require any modification to the chassis and can quickly multiply the copy number of BGC through one-step integration [30]. Accordingly, we set to further increase di-AFN A_1 production by augmenting the copy number of the whole BGC.

Given that the pPAB backbone already has a φC31-*attP*$^{\varphi C31}$ system, we chose the other two integrase systems, VWB1-*attP*^{VWB1} [31] and TG1-*attP*^{TG1} [32] and inserted these two integrase cassettes into plasmid pPAB_afn2 to generate pPVTAB_afn3 (Fig. 3A). The resultant plasmid was conjugated into *S. lividans* TK24 to generate *S. livi*/afn3. We randomly picked eight ex-conjugates to verify the integration efficiency and found that five clones had all three designated copies of the di-AFN A_1 BGC (Fig. 3B). Then, the correct *S. livi*/afn3 strains were fermented for five days and analyzed by HPLC. The AFN A_1 yield in *S. livi*/afn3 was 3.40 ± 0.47 mg·L^{-1}, which was slightly higher than that in *S. livi*/afn2 containing one di-AFN A_1 cluster, while the titer of di-AFN A_1 was 0.36 ± 0.04 mg·L^{-1}, which is a little bit lower than that in *S. livi*/afn2 (Fig. 3D).

Such a phenomenon that the product yield is not increased as its BGC is multiplied has been observed [33]. One possible explanation is that the exogenous BGCs impose high pressure to the host and greatly influence its metabolism. In addition, since the promoters used in this study are all strong

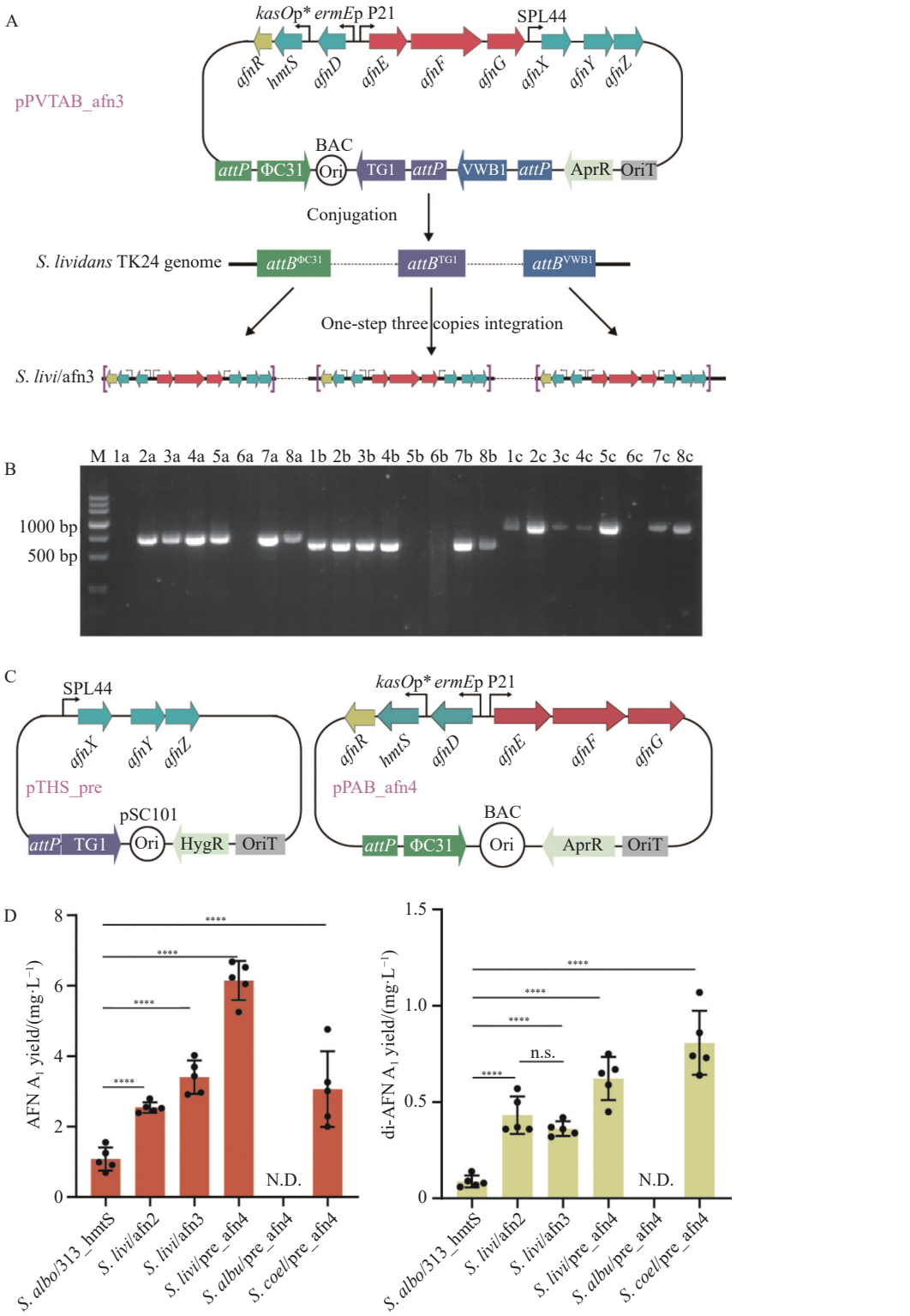

Fig. 3 Increasing the di-AFN A_1 yield by different strategies. (A) Schematic representation of multiplying the copy number of the di-AFN A_1 BGC by the *Att/Int* systems. Three integrase systems, φC31-*attP*$^{\varphi C31}$, VWB1-*attP*^{VWB1}, and TG1-*attP*^{TG1} were inserted into plasmid pPVTAB_afn3. (B) PCR verification of the copy number of the di-AFN A_1 BGC integrated on *S. lividans* TK24 genome. M, marker; Lanes 1a−8a, and Lanes 1b−8b, and Lanes 1c−8c, verification of the integration of the di-AFN A_1 BGC at the sites of *attB*$^{\varphi C31}$, *attB*^{VWB}, and *attB*^{TG1}, respectively, for eight clones. Clones 2/3/4/7/8 are correct ones with three integrated di-AFN A_1 BGCs. (C) Illustration of splitting the di-AFN A_1 BGC into two plasmids. (D) Titers of AFN A_1 and di-AFN A_1 in different *Streptomyces* strains. Data are represented as the mean ± SD of five replicate experiments, ** means $P < 0.0001$, n.s. indicates non-significance, N.D. means not detected**

constitutive ones dependent on the same housekeeping sigma factor HrdB, including *ermE*p [34] and *ermE*p derived P21 [35], *kasO*p* [36] and *kasO*p* derived SPL44 [37], three-fold more promoters will compete for the limited number of RNA polymerase core enzymes, which may be unfavorable for the maintaining of robust expression of the di-AFN A_1 biosynthetic pathway.

Splitting of the BGC to improve di-AFN A_1 titer

We noticed that the Piz biosynthetic gene cassette that containing a *ktzI* and a *ktzT* homologues is located within the BGCs of almost all natural products with Piz moieties, including the BGCs of kutznerides, matlystatins, padanamides, himastatins, and sanglifehrins [38]. Moreover, bioinformatic analysis showed that more than 80 Piz biosynthetic gene cassettes were found within the predicted gene clusters [39]. Therefore, the *afn* gene cluster is very special with its NRPS genes, 6-Cl-L-Trp synthesis gene, and the Piz gene cassette separated to three sites on the genome of *S. alboflavus* 313, which inspired us to split the BGC for better production of di-AFN A_1.

As shown in Fig. 3C, the di-AFN A_1 BGC is split into two plasmids. The pPAB_afn4 plasmid with a φC31-*attP*$^{\varphi C31}$ integration system kept the four AFN A_1 biosynthetic genes (*afnD/E/G/H*) and the *hmtS* gene for coupling two AFN A_1s to di-AFN A_1. The pTHS_pre plasmid with a TG1-*attP*^{TG1} integration system was used for supplying the non-proteinogenic amino acids, 6-Cl-L-Trp and Piz. These two plasmids were introduced into *S. lividans* TK24 to generate *S. livi*/pre_afn4. Specifically, the titer of AFN A_1 in *S. livi*/pre_afn4 was improved to 6.15 ± 0.56 mg·L^{-1}, about 2.4-fold of that in *S. livi*/afn2, while the titer of di-AFN A_1 in *S. livi*/pre_afn4 was 0.62 ± 0.11 mg·L^{-1}, about 1.4-fold of that in the *S. livi*/afn2 and 6.9-fold of that in *S. albo*/313_hmtS (Fig. 3D).

Expression of the di-AFN A_1 BGC in different Streptomyces hosts

In addition to *S. lividans*, *S. coelicolor* M1154 and *S. albus* J1074 are also frequently used model strains for heterologous expression [40]. Then, we sequentially introduced the pPAB_afn4 and the pTHS_pre plasmids into *S. albus* J1074 and *S. coelicolor* M1154 to generate *S. albu*/pre_afn4 and *S. coel*/pre_afn4, respectively. There was no AFN A_1 or di-AFN A_1 production in *S. albu*/pre_afn4 (Fig. 3D). For *S. coel*/pre_afn4, the titer of AFN A_1 (3.06 ± 1.08 mg·L^{-1}) was much lower than that in *S. livi*/pre_afn4, while the titer of di-AFN A_1 (0.81 ± 0.17 mg·L^{-1}) was considerably higher than that in *S. livi*/pre_afn4 (Fig. 3D), suggesting that *S. coelicolor* M1154 is a more suitable host strain for di-AFN A_1 production. According to Fig. 3D, part of AFN A_1 has not been converted to di-AFN A_1, suggesting that the catalytic efficiency of the P450 enzyme HmtS is insufficient, and we might need to further enhance the yield of di-AFN A_1 through mining or engineering more effective P450 enzymes [41].

Conclusion

To construct a better strain for di-AFN A_1 production, we collected the genes for AFN A_1 biosynthesis and the coupling enzyme gene *hmtS*. We noticed that the AFN A_1 synthesis genes scatter at three sites on the genome of *S. alboflavus* 313, which is unusual for NRPS gene clusters. Heterologous production of di-AFN A_1 was first achieved by putting the AFN A_1 synthesis genes (*afnD/E/F/G/X/Y/Z*) and *hmtS* in one plasmid, before introduction into a model strain *S. lividans* TK24, where the titer of di-AFN A_1 was about 3.8-fold higher than that in *S. albo*/313_hmtS. In addition, the di-AFN A_1 BGC was multiplied and splitted to mimic the natural *afn* biosynthetic genes, and the di-AFN A_1 yield significantly increased by the later strategy. In *S. livi*/pre_afn4, the titer of di-AFN A_1 was 0.62 ± 0.11 mg·L^{-1}, about 6.9-fold higher than that in *S. albo*/313_hmtS. When testing different host strains, we found that the titer of di-AFN A_1 achieved 0.81 ± 0.17 mg·L^{-1} in *S. coel*/pre_afn4, about 8.0-fold higher than that in *S. albo*/313_hmtS, which will certainly facilitate the efforts of drug development of di-AFN A_1. Moreover, there are many well-developed genetic tools for the model strains *S. lividans* TK24 and *S. coelicolor* M1154. Heterologous production of di-AFN A_1 in these two hosts will set a solid foundation for further titer improvement and manipulation of the *afn* cluster to generate more di-AFN A_1 analogs.

References

[1] Mouncey NJ, Otani H, Udwary D, *et al*. New voyages to explore the natural product galaxy [J]. *J Ind Microbiol Biotechnol*, 2019, **46**(3-4): 273-279.

[2] Süssmuth RD, Mainz A. Nonribosomal peptide synthesis-principles and prospects [J]. *Angew Chem Int Ed Engl*, 2017, **56**(14): 3770-3821.

[3] Newman DJ, Cragg GM. Natural products as sources of new drugs over the nearly four decades from 01/1981 to 09/2019 [J]. *J Nat Prod*, 2020, **83**(3): 770-803.

[4] Guo ZY, Shen L, Ji ZQ, *et al*. NW-G01, a novel cyclic hexadepsipeptide antibiotic, produced by *Streptomyces alboflavus* 313: I. Taxonomy, fermentation, isolation, physicochemical properties and antibacterial activities [J]. *J Antibiot*, 2009, **62**(4): 201-205.

[5] Ji ZQ, Wei SP, Fan LX, *et al*. Three novel cyclic hexapeptides from *Streptomyces alboflavus* 313 and their antibacterial activity [J]. *Eur J Med Chem*, 2012, **50**: 296-303.

[6] Fan LX, Ji ZQ, Guo ZY, *et al*. NW-G12, a novel nonchlorinated cyclohexapeptide from *Streptomyces alboflavus* 313 [J]. *Chem Nat Compd*, 2013, **49**: 910-913.

[7] Guo ZY, Li P, Chen GZ, *et al*. Design and biosynthesis of dimeric alboflavusins with biaryl linkages *via* regiospecific C-C bond coupling [J]. *J Am Chem Soc*, 2018, **140**(51): 18009-18015.

[8] Oelke AJ, Antonietti F, Bertone L, *et al*. Total synthesis of chloptosin: a dimeric cyclohexapeptide [J]. *Chem Eur J*, 2011, **17**(15): 4183-4194.

[9] D'Angelo KA, Schissel CK, Pentelute BL, *et al*. Total synthesis of himastatin [J]. *Science*, 2022, **375**(6583): 894-899.

[10] Kim Y, Li CJ. Perspectives on green synthesis and catalysis [J]. *Green Synth Catal*, 2020, **1**: 1-11.

[11] Ng IS, Ye CM, Zhang ZX, *et al*. Daptomycin antibiotic production processes in fed-batch fermentation by *Streptomyces roseosporus* NRRL11379 with precursor effect and medium optimization [J]. *Bioprocess Biosyst Eng*, 2014, **37**(3): 415-423.

[12] McIntyre JJ, Bull AT, Bunch AW. Vancomycin production in

batch and continuous culture [J]. *Biotechnol Bioeng*, 1996, **49**(4): 412-420.
[13] Do CB, Mahabhashyam MS, Brudno M, *et al*. Probcons: probabilistic consistency-based multiple sequence alignment [J]. *Genome Res*, 2005, **15**(2): 330-340.
[14] Jiang WJ, Zhu TF. Targeted isolation and cloning of 100-kb microbial genomic sequences by Cas9-assisted targeting of chromosome segments [J]. *Nat Protoc*, 2016, **11**(5): 960-975.
[15] Jinek M, Chylinski K, Fonfara I, *et al*. A programmable dual-RNA-guided DNA endonuclease in adaptive bacterial immunity [J]. *Science*, 2012, **337**(6096): 816-821.
[16] Labun K, Montague TG, Krause M, *et al*. Chopchop v3: expanding the CRISPR web toolbox beyond genome editing [J]. *Nucleic Acids Res*, 2019, **47**(W1): W171-W174.
[17] Jiang WJ, Zhao XJ, Gabrieli T, *et al*. Cas9-assisted targeting of chromosome segments catch enables one-step targeted cloning of large gene clusters [J]. *Nat Commun*, 2015, **6**: 8101-8108.
[18] Kieser T, Bibb MJ, Buttner MJ, *et al*. *Practical Streptomyces genetics* [M]. Norwich: John Innes Foundation Norwich, 2000.
[19] Lou CB, Stanton B, Chen YJ, *et al*. Ribozyme-based insulator parts buffer synthetic circuits from genetic context [J]. *Nat Biotechnol*, 2012, **30**(11): 1137-1142.
[20] Salis HM, Mirsky EA, Voigt CA. Automated design of synthetic ribosome binding sites to control protein expression [J]. *Nat Biotechnol*, 2009, **27**(10): 946-950.
[21] Neumann CS, Jiang W, Heemstra JR, *et al*. Biosynthesis of piperazic acid *via* N^5-hydroxy-ornithine in *Kutzneria* spp. 744 [J]. *Chembiochem*, 2012, **13**(7): 972-976.
[22] Du YL, He HY, Higgins MA, *et al*. A heme-dependent enzyme forms the nitrogen-nitrogen bond in piperazate [J]. *Nature Chem Biol*, 2017, **13**(8): 836-838.
[23] Blin K, Shaw S, Kloosterman AM, *et al*. Antismash 6.0: improving cluster detection and comparison capabilities [J]. *Nucleic Acids Res*, 2021, **49**(W1): W29-W35.
[24] Peng QY, Gao GX, Lü J, *et al*. Engineered *Streptomyces lividans* strains for optimal identification and expression of cryptic biosynthetic gene clusters [J]. *Front Microbiol*, 2018, **9**: 3042-3046.
[25] Yin SL, Wang XF, Shi MX, *et al*. Improvement of oxytetracycline production mediated *via* cooperation of resistance genes in *Streptomyces rimosus* [J]. *Sci China Life Sci*, 2017, **60**(6): 992-999.
[26] Yanai K, Murakami T, Bibb M. Amplification of the entire kanamycin biosynthetic gene cluster during empirical strain improvement of *Streptomyces kanamyceticus* [J]. *Proc Natl Acad Sci U S A*, 2006, **103**(25): 9661-9666.
[27] Murakami T, Burian J, Yanai K, *et al*. A system for the targeted amplification of bacterial gene clusters multiplies antibiotic yield in *Streptomyces coelicolor* [J]. *Proc Natl Acad Sci U S A*, 2011, **108**(38): 16020-16025.
[28] Li H, Pan YY, Liu G. Multiplying the heterologous production of spinosad through tandem amplification of its biosynthetic gene cluster in *Streptomyces coelicolor* [J]. *Microb Biotechnol*, 2022, **15**(5): 1550-1560.
[29] Li L, Wei K, Liu X, *et al*. aMSGE: advanced multiplex site-specific genome engineering with orthogonal modular recombinases in actinomycetes [J]. *Metab Eng*, 2019, **52**: 153-167.
[30] Li L, Liu XC, Wei KK, *et al*. Synthetic biology approaches for chromosomal integration of genes and pathways in industrial microbial systems [J]. *Biotechnol Adv*, 2019, **37**(5): 730-745.
[31] Van ML, Mei LJ, Lammertyn E, *et al*. Site-specific integration of bacteriophage VWB genome into *Streptomyces venezuelae* and construction of a VWB-based integrative vector [J]. *Microbiology*, 1998, **144**(12): 3351-3358.
[32] Morita K, Yamamoto T, Fusada N, *et al*. The site-specific recombination system of actinophage TG1 [J]. *FEMS Microbiol Lett*, 2009, **297**(2): 234-240.
[33] Li L, Zheng GS, Chen J, *et al*. Multiplexed site-specific genome engineering for overproducing bioactive secondary metabolites in actinomycetes [J]. *Metab Eng*, 2017, **40**: 80-92.
[34] Bibb MJ, White J, Ward JM, *et al*. The mRNA for the 23s rRNA methylase encoded by the *ermE* gene of *Saccharopolyspora erythraea* is translated in the absence of a conventional ribosome-binding site [J]. *Mol Microbiol*, 1994, **14**(3): 533-545.
[35] Siegl T, Tokovenko B, Myronovskyi M, *et al*. Design, construction and characterisation of a synthetic promoter library for fine-tuned gene expression in actinomycetes [J]. *Metab Eng*, 2013, **19**: 98-106.
[36] Wang W, Li X, Wang J, *et al*. An engineered strong promoter for *Streptomycetes* [J]. *Appl Environ Microbiol*, 2013, **79**(14): 4484-4492.
[37] Bai CX, Zhang Y, Zhao XJ, *et al*. Exploiting a precise design of universal synthetic modular regulatory elements to unlock the microbial natural products in *Streptomyces* [J]. *Proc Natl Acad Sci U S A*, 2015, **112**(39): 12181-12186.
[38] Morgan KD, Andersen RJ, Ryan KS. Piperazic acid-containing natural products: structures and biosynthesis [J]. *Nat Prod Rep*, 2019, **36**(12): 1628-1653.
[39] Hu Y, Qi Y, Stumpf SD, *et al*. Bioinformatic and functional evaluation of actinobacterial piperazate metabolism [J]. *ACS Chem Biol*, 2019, **14**(4): 696-703.
[40] Huo LJ, Hug JJ, Fu CZ, *et al*. Heterologous expression of bacterial natural product biosynthetic pathways [J]. *Nat Prod Rep*, 2019, **36**(10): 1412-1436.
[41] Li RJ, Zhang Z, Acevedo-Rocha CG, *et al*. Biosynthesis of organic molecules *via* artificial cascade reactions based on cytochrome p450 monooxygenases [J]. *Green Synth Catal*, 2020, **1**(1): 52-59.

Cite this article as: WEI Weijia , WANG Wenzhao , LI Chao , TANG Yue , GUO Zhengyan , CHEN Yihua . Construction and heterologous expression of the di-AFN A_1 biosynthetic gene cluster in *Streptomyces* model strains [J]. *Chin J Nat Med*, 2022, **20**(11): 873-880.